Protoplasma 124, 137—146 (1985)

PROTOPLASMA

Euglenoid Movement in *Euglena fusca*: Evidence for Sliding Between Pellicular Strips

Brief Report

T. SUZAKI and R. E. WILLIAMSON*

Department of Developmental Biology, Research School of Biological Sciences, The Australian National University, Canberra

Received June 1, 1984
Accepted July 31, 1984

Summary

In *Euglena fusca*, each pellicular strip carries a row of particles on its surface. The relative displacement of particles on adjacent strips was analysed by video-microscopy and evidence was obtained that adjacent pellicular strips slide relative to each other during euglenoid movement. *E. fusca* shows two types of euglenoid movement, oscillatory bending and rounding-up of the cell body. During oscillatory bending, the maximum velocity of sliding was 0.4 μm/s and the maximum displacement distance between adjacent strips 2.3 μm about their mean position. When *E. fusca* exhibited rounding-up of the cell body, particle displacement again occurred and the angle of the pellicular strips to the long axis of the cell body increased because of pellicular sliding. As a result the distance between the cell's anterior and posterior tips was reduced. There was no change in distance either between rows of particles or between particles within the same row. The findings are incompatible with theories of euglenoid movement requiring local contraction of pellicular strips and point to the likely existence of active sliding between adjacent strips.

Keywords: Euglena fusca; Euglenoid movement; Flagellate; Microtubules; Videomicroscopy.

1. Introduction

Euglenoid movement or metaboly is the characteristic motility of euglenoid flagellates and was first noted by HARRIS in 1696. It is defined as a change in cell shape (PRINGSHEIM 1948) and is known to play important roles in several different cell functions.

Cell body contraction enables *Euglena* to change the direction of its swimming movement (LOWNDES 1936, MIKOLAJCZYK 1972, BOVEE 1982) while in gliding euglenoids, body contraction serves both for locomotion and for changing the direction of gliding (HALL 1931, BRACHER 1938, CHEN 1950, HILMBAUER 1954, MACKINNON and HAWES 1961, MIKOLAJCZYK 1975, MIKOLAJCZYK and KUZNICKI 1981). In other species, euglenoid movement is also involved in exiting from the cyst (BOVEE 1982) or test (HILMBAUER 1954) and in wiggling in and out through the cuticle or shell of a food organism (BOVEE 1982). Furthermore, phototaxis of gliding *Euglena* was recently found to be generated by controlled changes in body shape (HÄDER and MELKONIAN 1983).

Although the mechanism of euglenoid movement is still unknown, many investigators have assumed that the structures responsible for it are located within the pellicular complex (DISKUS 1956, DASGUPTA 1964, JAHN and BOVEE 1964, ARNOTT and WALNE 1966, ARNOTT and SMITH 1969, SCHWELITZ *et al.* 1970, MIKOLAJCZYK 1973, HOFMANN and BOUCK 1976, MIKOLAJCZYK and KUZNICKI 1981). LEEDALE (1964, 1966) stated that the pellicular strips of *E. spirogyra* move against each other during euglenoid movement but no evidence was presented regarding this important point. For this reason, we have examined *E. fusca*, a relatively large species (100–200 μm in length) with many ornamenta-

* Correspondence and Reprints: Department of Developmental Biology, Research School of Biological Sciences, The Australian National University, PO Box 475, Canberra City, ACT, 2601, Australia.

tion particles on the cell surface which can be easily traced under a light microscope. In the present study, we employed these particles as intrinsic cell surface markers to monitor relative movements of the pellicular strips. Evidence was obtained which shows that adjacent pellicular strips move against each other when the cell changes its shape.

2. Materials and Methods

Euglena fusca was a generous gift of Professor M. SAITO (Yokohama National University), who initially collected the species at Yokohama, Japan. The cells were grown in biphasic culture (PRINGSHEIM 1946) at 26 °C in a light-dark cycle of 12 and 12 hours.

Living cells were examined with a Zeiss microscope equipped with Nomarski intereference optics and a video system. The output of the video camera with Newvicon tube (Model 65, Dage-MTI, Inc.) was fed through a video processor (Model 604, Colorado Video Inc.) and a time-date generator (VTG-33, FOR-A Co., Ltd.) to a ¾-inch cassette video tape recorder (SONY VO-5800 PS). Movement and location of the surface particles was monitored using frame by frame analysis of the tape record and a position analyser (VPA-1000, FOR-A Co., Ltd.).

Material for electron microscopy was fixed at room temperature with 3% glutaraldehyde in 25 mM phosphate buffer (pH 7.0) for 30 minutes followed by 1% OsO_4 in the same buffer for 1 hour, and dehydrated in an acetone series. For transmission electron microscopy, fixed cells were embedded in Spurr's resin (SPURR 1969). Thin sections were stained with 10% uranyl acetate in 50% ethanol for 10 minutes and lead citrate (REYNOLDS 1963) for 3 minutes, and examined in a Hitachi H600 electron microscope. For scanning electron microscopy, cells were critical point dried with CO_2, sputter coated with Au, and observed with a Cambridge Stereoscan S 180 scanning electron microscope.

3. Results

3.1. Surface Structure of E. fusca

The swimming *E. fusca* usually exhibits a slender rod-like cell shape and each pellicular strip carries a single row of particles (Figs. 1–5). The rows may run almost parallel to the long axis of the cell (Fig. 1) or be slightly coiled in a left-handed manner (Fig. 3). The rows lie closer and the particles are differently shaped where the cell tapers at its extremities. In the midregion of the cell, each particle is triangular in shape when viewed from above, with the base of the triangle parallel to the striations that mark the junction of adjacent strips (Figs. 2–4). Each particle is composed of small granules about 0.1 μm in diameter, which gather to make a crown-like configuration when viewed from the side (Fig. 5). They are attached directly to the plasma membrane (Fig. 7, arrowhead) under which are the interlocking pellicular strips (Fig. 6, *s*), each 0.1–0.3 μm thick and about 3 μm wide. Beneath each pellicular strip, three microtubules lie parallel to the direction of the surface striations (Fig. 7, arrows). Two microtubules are located at the groove region between adjacent strips while the third is on the other side of the strip. Electron dense projections (Fig. 8, arrowheads) protrude from the upper surface of each pellicular strip towards the lower surface of the adjacent one and might correspond to the "teeth" structure of *E. spirogyra* (LEEDALE 1964). Tubular endoplasmic reticulum (cisternae about 50 nm in diameter) was often observed between these projections (Fig. 8, arrows).

3.2. Bending Movement

Euglenoid movement was induced by slightly compressing the cell between a slide and coverslip. Oscillatory bending movement of the cell was most often observed (Fig. 9), especially when the pellicular striations were running parallel to the cell axis. (The term: "oscillatory bending" is purely descriptive and no relationship to the "oscillatory movements" of certain blue green algae is implied.) The cell sometimes showed twisting and rounding-up movements as well. One cycle of the bending movements (Figs. 9 *a–h*) lasted about 20–30 seconds, with anterior and posterior parts of the cell always bending towards different sides of the cell body.

Changes in the position of the surface particles were examined on video records. Measurements were made initially on particles located in the middle part of the cell above the nucleus (light ellipses in Fig. 9). The longitudinal component of the distance between a pair of particles located on adjacent rows was first calculated at time 0 from the coordinate of each particle (X_0 in Fig. 10). The longitudinal displacement of the particles during time t was then calculated as the difference between the value obtained at time 0 (X_0) and after time t (X_t). Measurements and calculations were repeated at 2 second intervals. Fig. 11 shows the displacement of particles in adjacent rows as a function of time (*b*) and its differential transform (*c*), the sliding velocity. Adjacent rows of particles were found to be displaced against each other in a cyclic manner with the same period as for the overall cell shape change. The maximum displacement of the adjacent strips was roughly 1.5 μm about their mean position, with greatest displacement occurring when the cell was maximally deformed (shaded drawings in Fig. 11 *a*). The sliding velocity was maximal (about 0.4 μm/second) when the cell shape became elongated, roughly midway between these states of maximum deformation. When the

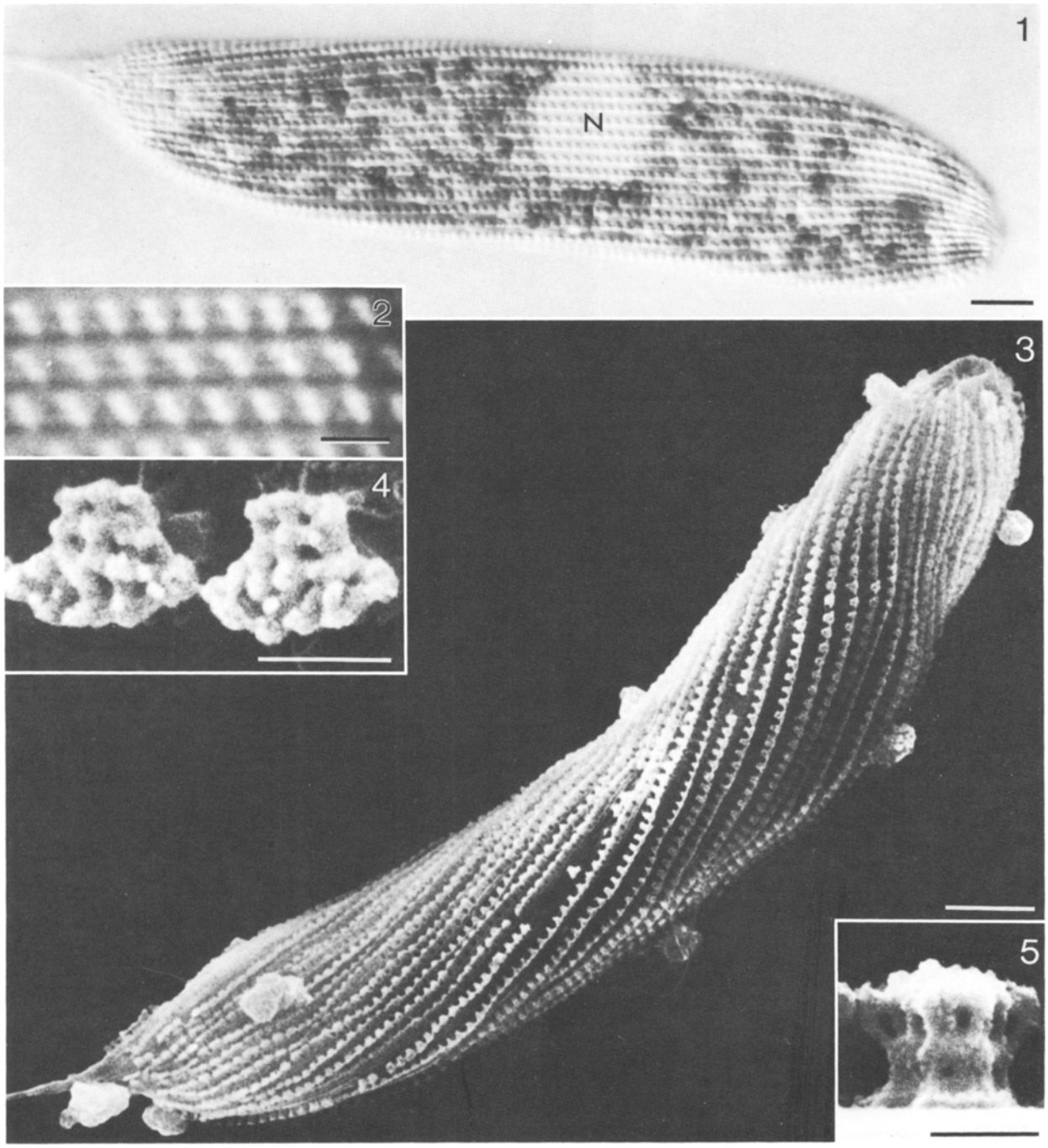

Fig. 1. Light micrograph of a living *E. fusca* cell showing the whole cell body with rows of surface particles running almost parallel to the long axis of the cell. Anterior tip is on the right side of the micrograph. *N* nucleus. × 980. Bar = 10 μm

Fig. 2. Light micrograph of a highly magnified region of the cell surface in the midregion of a cell over the nucleus and showing the triangular shape of the surface particles. × 5,400. Bar = 2 μm

Figs. 3–5. Scanning electron micrographs of *E. fusca*. Fig. 3. Cell with pellicular strips slightly twisted in left-handed manner. × 1,400. Bar = 10 μm. Fig. 4. Surface particles viewed from above. × 21,000. Bar = 1 μm. Fig. 5. Side view of a surface particle. × 17,000. Bar = 1 μm

longitudinal displacement between particles in adjacent rows was measured in various parts of the cell, the maximum displacement during one cycle of bending was found to be a function of position along the cell's length (Fig. 12). Displacements were greatest in the middle of the cell and approached zero at both ends. The distance between adjacent particles within a single row was also measured in different regions of one cell during bending movement. As shown in Fig. 13, there were no significant changes in inter-particle spacings.

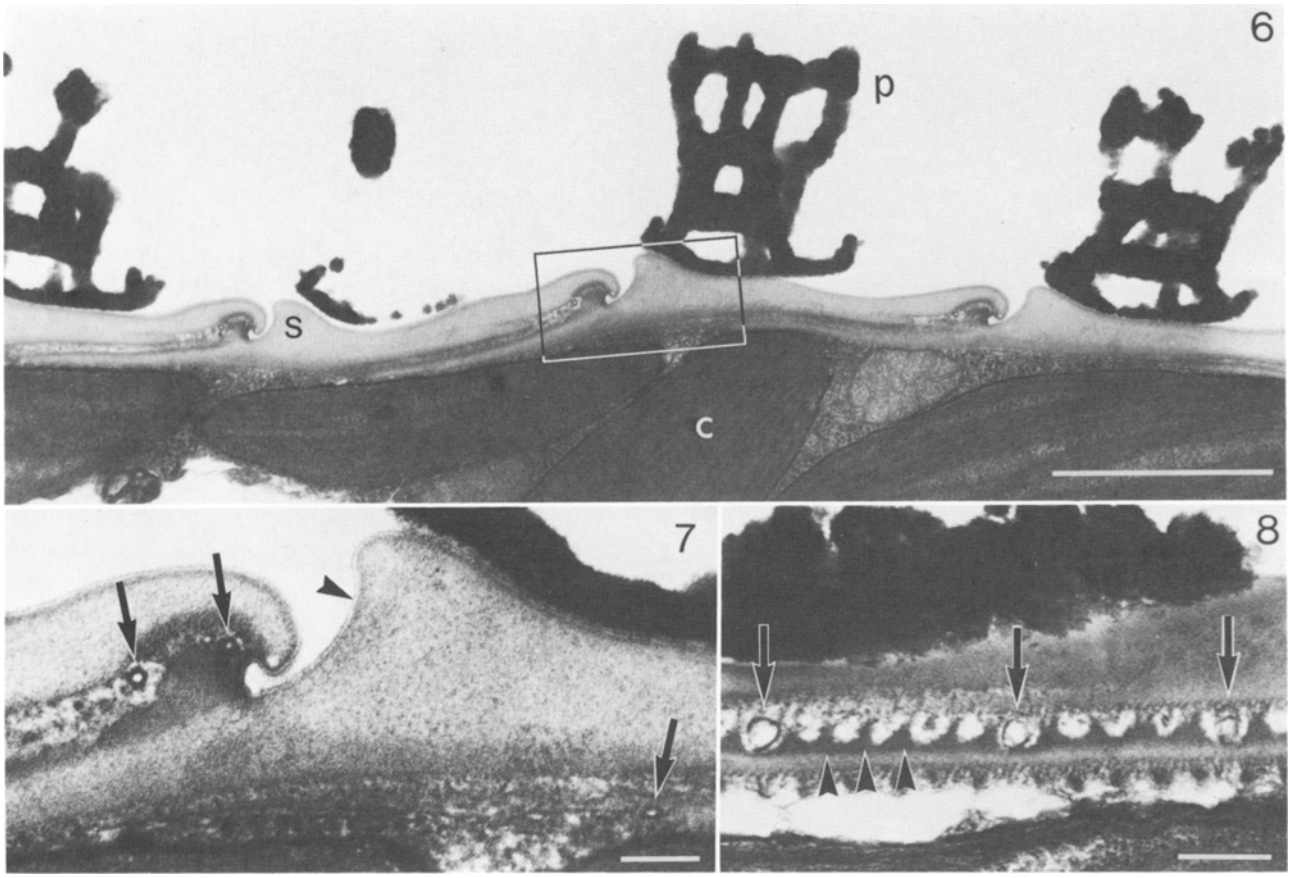

Figs. 6–8. Transmission electron micrographs of surface structure of *E. fusca*. Fig. 6. Low magnification picture of a cross-section of cell cortex with surface particles (*p*), interlocking pellicular strips (*s*), and chloroplasts (*c*). × 29,000. Bar = 1 μm. Fig. 7. Highly magnified picture of the area enclosed in Fig. 6, showing three microtubules (arrows) and the plasma membrane (arrowhead). × 100,000. Bar = 100 nm. Fig. 8. Longitudinal section of pellicular structures cut in a plane perpendicular to that of the cross-sectional view in Figs. 6 and 7. Electron-dense projections (arrowheads) and tubular endoplasmic reticulum (arrows) are present. × 61,000. Bar = 200 nm

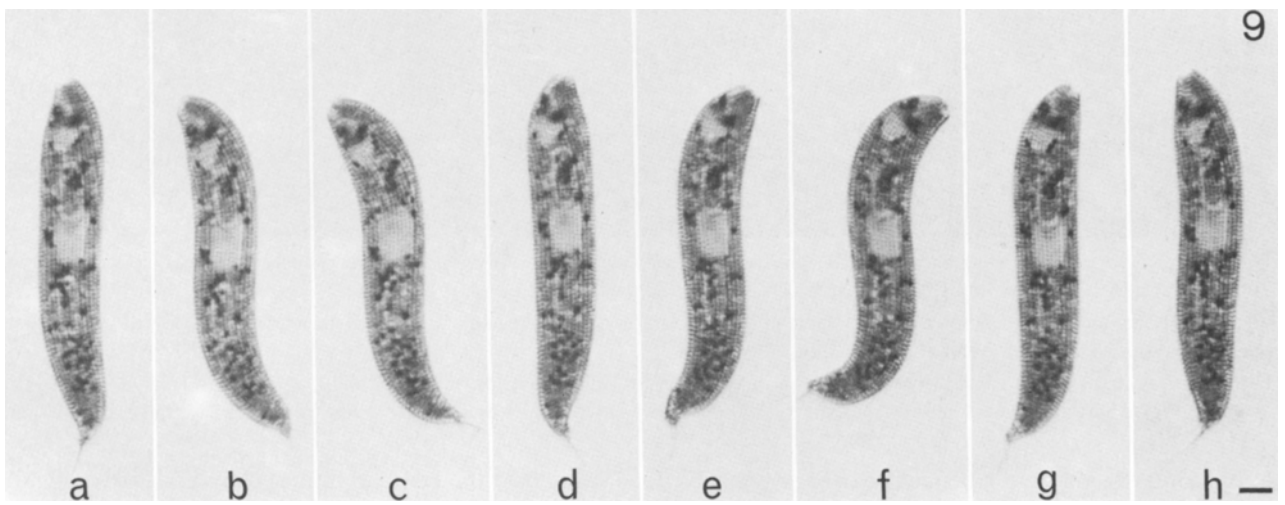

Fig. 9. Sequential light micrographs of *E. fusca* during bending motion induced by compressing the cell between a slide and coverslip. Pictures (*a*) to (*h*) were taken at 4-second intervals. × 410. Bar = 10 μm

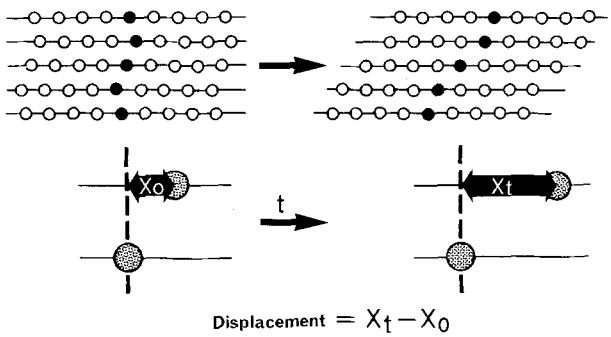

Fig. 10. Diagram representing the procedure for measurement and calculation of displacement between adjacent rows of surface particles. See the text for details

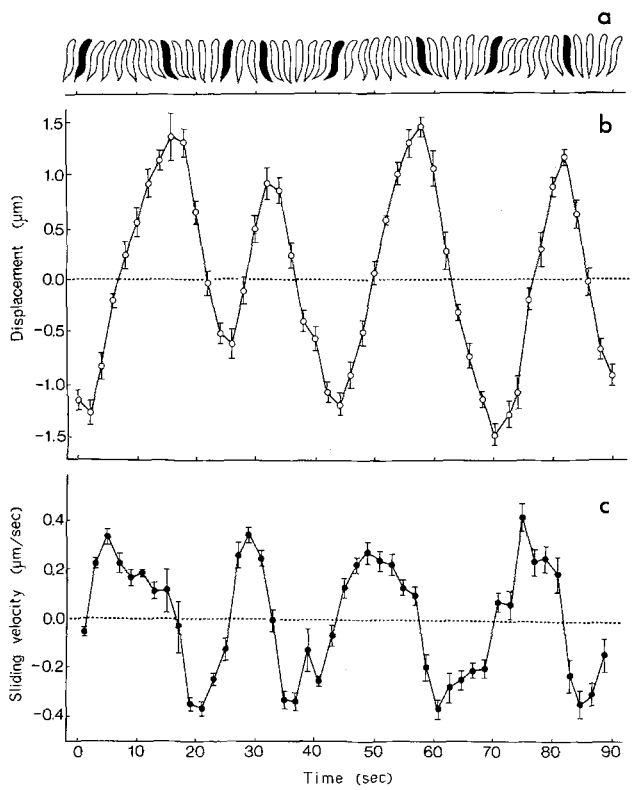

Fig. 11. Change in cell shape (*a*), displacement between adjacent rows of particles above the nucleus (*b*), and sliding velocity (*c*) all as a function of time for one cell undergoind oscillatory bending. Mean values for 6 pairs of rows and standard errors (n = 6) are plotted in *b* and *c*. Outlines of the cell shape were traced directly from the TV monitor screen. Sliding velocity was calculated from the change in displacement between successive times. A mean value was calculated from all of the obtained figures for displacement (46 points in about 4 cycles of cell shape change), and all values were normalized as differences from the mean value (zero line in *b*)

3.3. Rounding-Up of the Cell Body

E. fusca sometimes exhibited rounding-up of the cell body in the same conditions in which oscillatory bending was observed. Fig. 14 shows the appearance of the same cell before and after rounding-up. Flattening

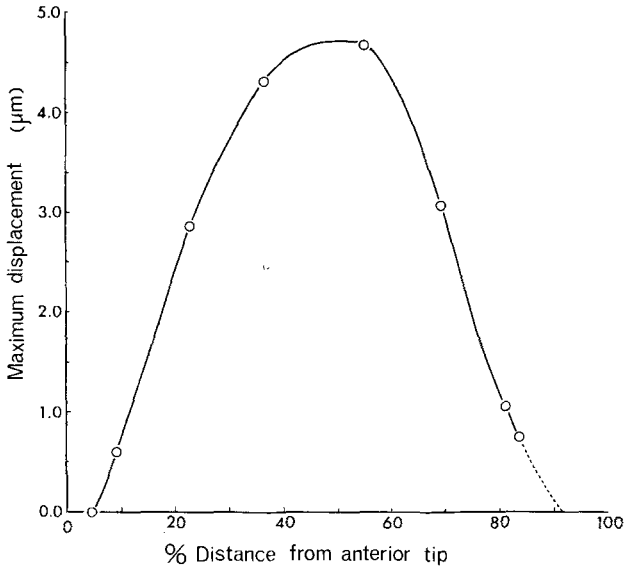

Fig. 12. Relationship between the maximum displacement of rows of particles and their position on the cell surface. Relative displacement of particles in adjacent rows was measured in different parts of a cell using the method shown in Figs. 10 and 11. The maximum displacement during one cycle of bending movement was then plotted against % distance from the anterior tip. The scarcity of particles precludes accurate measurements at the posterior tip (see Figs. 1 and 3)

of the cell in the dorsi-ventral direction always accompanied rounding-up, so that the rounded cell resembled a flat disc. During cell rounding-up, the rows of particles again exhibited relative displacement but changes in focal plane precluded the collection of adequate video records for detailed analysis. The pellicular striations, which were initially almost parallel to the cell axis (Fig. 14 *a*), gradually tilted away from the long axis of the cell body until their orientation to the cell axis usually exceeded 45° when the cell was fully rounded-up (maximum angle is about 65° in Fig. 14 *b*). The distance between neighboring rows of surface particles and between adjacent particles within the same row were measured in the middle region of elongated and rounded cells. As shown in Tab. 1, there was no significant difference in either parameter. The anterior region of a partially rounded cell (Fig. 15) shows some distinctive details of the surface structure. Here the pellicular strips and their particles taper and are coiled in a left-handed manner. As in all other parts of the cell surface, however, one edge of each triangular-shaped particle has remained parallel to the striations marking the junction of adjacent strips.

4. Discussion

There are 5 main findings from our video analysis of the surface particle movements that accompany cell shape

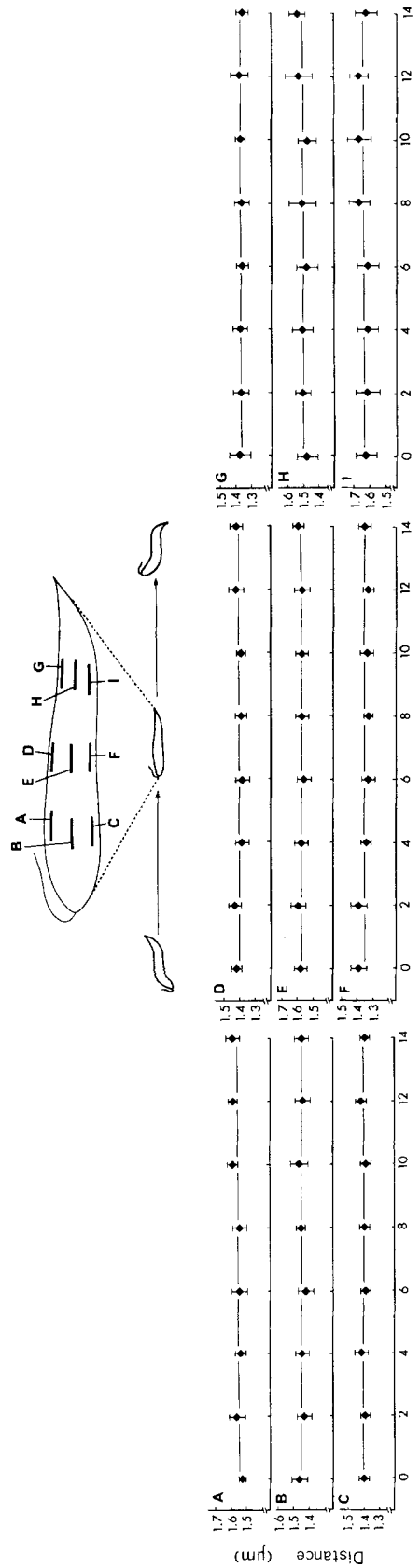

Fig. 13. Change in inter-particle spacing during bending movement. The locations of 10 sequential particles within individual rows were traced, and mean values for their spacing are plotted with standard deviations. Measurements were carried out at 9 different regions of one cell. Outlines of the cell shape and the position of the rows of particles used for measurement are also shown at the top of the graphs

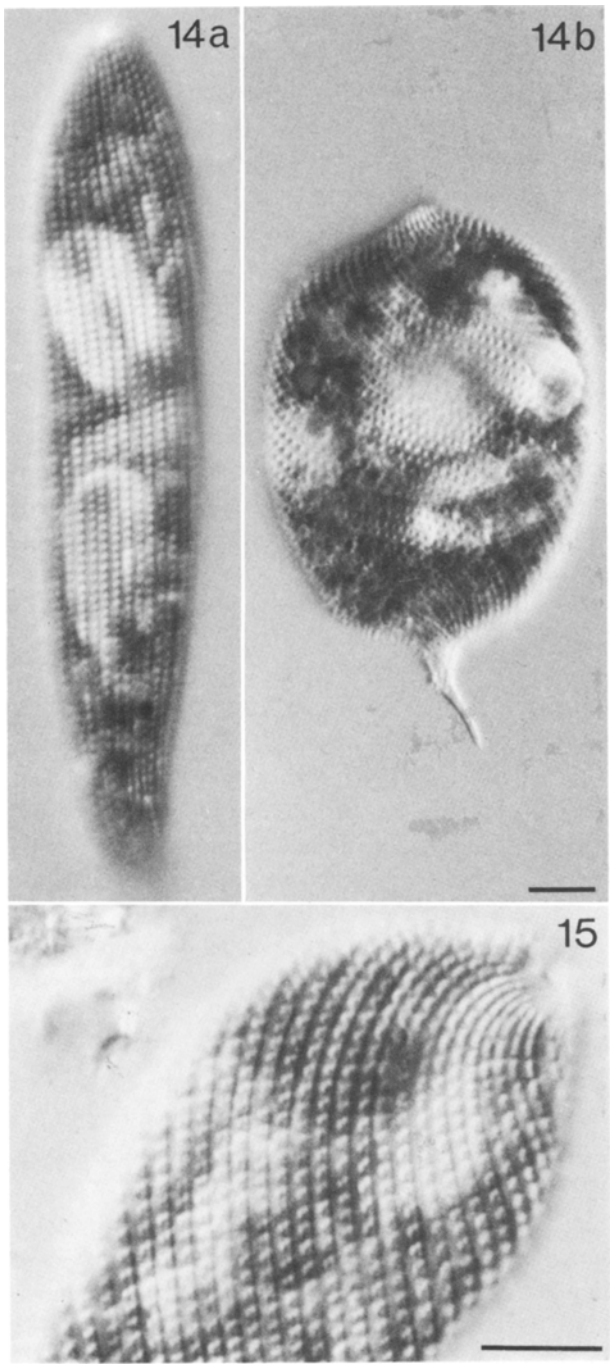

Fig. 14. Light micrographs of the same cell before (*a*) and after (*b*) rounding-up movement. Rounding-up of the cell involves both a change in the angle of pellicular striations to the long axis and a twisting motion of the cell body. × 830. Bar = 10 μm

Fig. 15. Anterior region of a partially rounded cell. One of the edges of each particle is always aligned parallel to the direction of the surface striation, although the striations are undergoing bending and twisting on the cell surface. × 1,600. Bar = 10 μm

Table 1. *Separation distances between particles within a row and between adjacent rows of particles before and after rounding up*[1]

	Distances between adjacent particles within a row (μm)	Distance between adjacent rows of particles (μm)
Elongated	1.61 ± 0.08	2.00 ± 0.21
Rounded-up[2]	1.60 ± 0.08	1.97 ± 0.18

[1] Measurements (20 per cell) were made at the middle region of 20 cells in each of the stages of cell shape change. Mean values and standard deviations are shown in the table.
[2] Cells having surface striations tilted > 45° to the axis of the cell body.

changes in *E. fusca*. 1. Particles in adjacent strips are displaced relative to each other during bending and rounding-up. 2. The maximum displacement during bending is a function of position along the cell, being maximal in the midregion and approaching zero at both ends. 3. The spacing between the particles on one pellicular strip remains constant, even in regions of the cell that are bending. 4. The distance between rows of particles on adjacent strips similarly remains constant. 5. The base of each triangular particle remains parallel to the striation marking the junction of adjacent pellicular strips. These observations can be used to infer some important dynamic properties of the pellicle and to exclude certain theories of euglenoid movement. Three mechanisms able to cause the cell shape changes seen during oscillatory bending are summarized in Fig. 16 together with the expected behavior of the surface particles. The three models involve respectively localized contraction of the pellicular strips (Fig. 16, *A*), relative sliding of pellicular strips with minimum distortion (Fig. 16, *B*) and distortion of pellicular strips (Fig. 16, *C*).

Theories involving localized contraction of the pellicle (Fig. 16, A, KHAWKINE 1887, ARNOTT and SMITH 1969, SCHWELITZ *et al.* 1970, MIKOLAJCZYK 1973) can be discounted since no change in particle spacing is observed within rows and the observed displacement of particles in adjacent rows would not be expected. Contraction of a traversing fiber that connects adjacent strips in *E. gracilis* (MIKOLAJCZYK and KUZNICKI 1981) would reduce the separation between adjacent rows of particles without, since it runs transversely, producing longitudinal displacement. It too can therefore be discounted.

The relative displacement between particles in adjacent rows could arise either from sliding between adjacent

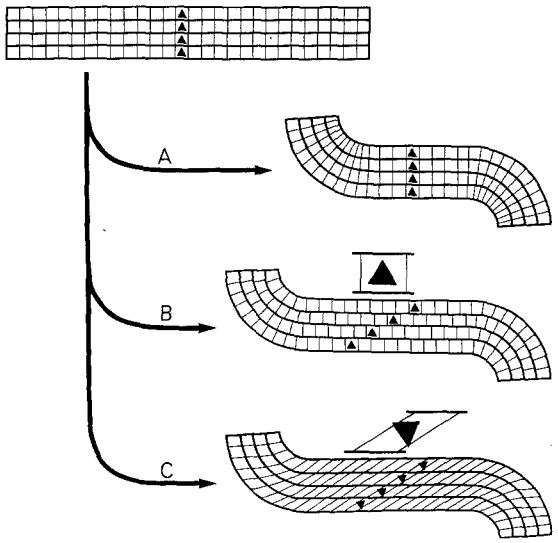

Fig. 16. Schematic diagrams representing three possible ways in which the pellicular strips might generate cell bending and the predicted behavior of surface particles on each model. The diagram on the top shows an elongated stage, with straight pellicular strips. *A* Cell bending occurs because strips contract in the bending regions. No sliding occurs. *B* Bending occurs without active contraction as a result of sliding between strips. The only changes in strip shape occur in the bends as a result not a cause of bending. *C* Bending occurs without sliding of strips as a result of strip distortion that is greatest in the middle region of the cell. Model *B* is favored for reasons discussed in the text

pellicular strips (Fig. 16, *B*) or from the distortion of individual strips that do not slide relative to their neighbors (Fig. 16 *C*). We favor sliding between adjacent strips since the large distortions required on model C have to take place without a change in the alignment of the surface particles with respect to the edge of the strips (see Fig. 15) and ultrastructural work shows that neither the regular particle array in the plasma membrane nor the alignment of various transversely oriented components of the pellicular strips show the deformation expected on this theory (manuscript in preparation). While we have distinguished the sliding model from others involving contraction (Fig. 16, *A*) and distortion (Fig. 16, *B*) of strips, the sliding strips in the regions where the cell bends must have their inner and outer edges respectively compressed and stretched until they differ in length by about 5%. These changes in strip shape are much less than the contractions required if sliding does not take place (Fig. 16, *A*) and, unlike the different type of changes in strip shape that are envisaged in the third model (Fig. 16, *C*), they are confined to those regions of strips lying in the areas of cell bending.

We believe therefore that the observed particle displacements result from sliding between adjacent strips that are anchored to prevent displacements at both the anterior and posterior ends (see the graph of displacement as a function of position along the cell, Fig. 12).

The critical question then is how the sliding is generated. The two basic possibilities are that sliding is active and generates the changes in cell shape or that sliding is passive and occurs to accomodate changes in cell shape that are generated by contractile activity deeper in the cytoplasm (LEEDALE 1964, 1966, 1982, LEEDALE *et al.* 1965). At the moment, the evidence is not available to distinguish firmly between these hypotheses. However, we may note that electron microscopy has not provided any indications of the cytoskeletal components (most plausibly actomyosin) that would occur deeper in the cytoplasm to generate the necessary force for the second model. Furthermore, cytochalasin B, a widely effective inhibitor of actomyosin-based motility (TANENBAUM 1978), does not inhibit euglenoid movement (HUXTABLE and HYAMS 1982). It is also difficult to explain bending and twisting movements of euglenoid cells by this hypothesis (GALLO and SHRÉVEL 1982). In contrast, there are at least two plausible ways in which components of the pellicular complex could generate active sliding between strips. These are microtubule-membrane sliding (GALLO and SHRÉVEL 1982) and direct interaction between adjacent pellicular strips where they approach in the groove region (Fig. 7). Microtubule-microtubule sliding as proposed for *E. gracilis* by HOFMANN and BOUCK (1976) seems less attractive in *E. fusca* where the microtubules are 100 nm apart [*cf.*, the 10–15 nm spacing of sliding microtubules in axonemes (WARNER 1978) and flagellate axostyles (BLOODGOOD and MILLER 1974)].

Because rounding-up also involved particle displacement, and intermediate stages between bending and rounding-up were observed, we believe that active sliding between pellicular strips may also underlie rounding-up. Although a detailed record of particle movements was not obtained, a simple geometric argument illustrates the feasibility of this idea by allowing calculation of the required sliding between strips. The theory requires that the strips do not change in length and width during rounding-up (Tab. 1) and that, as in bending movements (Fig. 13), the strips show no relative displacement at the ends of the cell. The theory was previously applied to the process of microtubule to macrotubule transformation in heliozoan axopodia (SUZAKI *et al.* 1980) where the increase in tubule diameter was considered to result from sliding

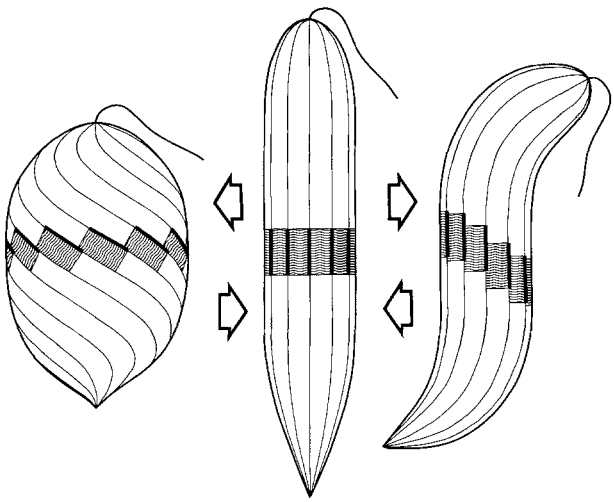

Fig. 17. Schematic diagrams of rounding-up and bending movements accompanied by relative sliding of the pellicular strips. When the cell rounds up, the sliding of pellicular strips would be expected to occur evenly while during bending motion, movements on upper and lower portions of the cell surface would exceed those at the sides. Short segments of the cell surface are shaded to emphasize the relative sliding motion between adjacent pellicular strips

between adjacent protofilaments. In *Euglena,* the displacement between strips (χ) is then given by:

$$\chi = d \tan \theta$$

where d is the distance between rows of particles (about 2.0 μm) and θ is the angle of the strips to the long axis of the cell. In Fig. 15, for example, maximum displacement has occurred in the middle part of the cell where θ is about 65° and χ is then calculated to be 4.1 μm. This is considerably bigger than the 1.5–2.3 μm displacement about the mean position recorded during oscillatory bending (Figs. 11 and 12). (Such large displacements, exceeding 2 particle spacings, pose even more severe problems for the previously discussed strip distortion model of Fig. 16, C).

A further difference between rounding-up and bending concerns the distribution of sliding over the cell's circumference. During rounding-up, sliding of the strips would be expected to occur quite evenly over the surface to cause the symmetrical shape transformation. In contrast, bending would require more sliding between adjacent strips on the upper and lower surfaces than between strips located on the sides of the cell (Fig. 17) where particle displacements have yet to be measured. Different patterns of cell movement might therefore depend both on the magnitude and the distribution of sliding between adjacent strips. The relevant control mechanisms are unknown.

In conclusion, analysis of surface particle movements in *E. fusca* shows that euglenoid movement is accompanied by the longitudinal displacement of particles on adjacent strips. The occurrence of active sliding between pellicular strips provides the most plausible explanation for this. The amplitude and distribution of sliding would determine whether bending or rounding-up resulted. Further work is being directed towards computer simulation of the shape changes to test the quantitative feasibility of such a model and to characterizing the mechanism and control of force generation using detergent-extracted cell models.

Acknowledgements

We thank Professor B. E. S. GUNNING and Dr. A. R. HARDHAM for their helpful discussion and for critical reading of the manuscript. One of us (T. SUZAKI) is grateful for the financial support of an ANU Scholarship.

References

ARNOTT, H. J., SMITH, H. E., 1969: Analysis of microtubule structure in *Euglena granulata.* J. Phycol. **5**, 68—75.

— WALNE, P. L., 1966: Metaboly in *Euglena granulata.* J. Phycol. **2** (Suppl.), 4—5 (Abstr.).

BLOODGOOD, R. A., MILLER, K. R., 1974: Freeze-fracture of microtubules and bridges in motile axostyles. J. Cell Biol. **62**, 660—671.

BOVEE, E. C., 1982: Movement and locomotion of *Euglena.* In: The biology of *Euglena,* Vol. 3 (BUETOW, D. E., ed.), pp. 143—168. New York: Academic Press.

BRACHER, R., 1938: The light relations of *Euglena limosa* Grad.— Part I. The influence of intensity and quality of light on phototaxy. J. Linn. Soc. London, Bot. **51**, 23—43.

CHEN, Y. T., 1950: Investigations on the biology of *Peranema trichophorum* (*Eugleninae*). Q. J. microsc. Sci. **91**, 279—308.

DASGUPTA, J., 1964: Submicroscopic morphology of *Euglena gracilis* Klebs. Ann. Sci. Nat. Zool. Biol. Anim. **6**, 215—227.

DISKUS, A., 1956: Färbestudien an den Schleimkörperchen und Schleimausscheidungen einiger Euglenen. Protoplasma **45**, 460—477.

GALLO, J.-M., SCHRÉVEL, J., 1982: Euglenoid movement in *Distigma proteus.* I. Cortical rotational motion. Biol. Cell **44**, 139—148.

HÄDER, D.-P., MELKONIAN, M., 1983: Phototaxis in the gliding flagellate, *Euglena mutabilis.* Arch. Microbiol. **135**, 25—29.

HALL, S. R., 1931: Obervations on *Euglena leucops,* sp. nov., a parasite of *Stenostomum,* with special reference to nuclear division. Biol. Bull. (Woods Hole, Mass.) **60**, 327—344.

HARRIS, J., 1969: Microscopical observations of vast numbers of animalcules seen in water. Philos. Trans. R. Soc. London Ser. B **19**, 254—259.

HILMBAUER, K., 1954: Zellphysiologische Studien an Euglenaceen, besonders an *Trachelomonas.* Protoplasma **43**, 192—227.

HOFMANN, C., BOUCK, B., 1976: Immunological and structural evidence for patterned intussusceptive surface growth in a unicellular organism. A postulated role for submembranous proteins and microtubules. J. Cell Biol. **69**, 693—715.

HUXTABLE, D. M., HYAMS, J. S., 1982: Euglenoid movement characterized by video light microscopy in *Euglena gracilis*. Brit. J. Phycol. **17**, 234 (Abstr.).

JAHN, T. L., BOVEE, E. C., 1964: Protoplasmic movements and locomotion of protozoa. In: Biochemistry and physiology of protozoa, Vol. 3 (HUTNER, S. H., ed.), pp. 61—129. New York: Academic Press.

KHAWKINE, W., 1887: Biology of *Astasia ocellata* and *Euglena viridis*. J. Roy. Microsc. Soc. Ser. II. **7**, 601—602.

LEEDALE, G. F., 1964: Pellicle structure in *Euglena*. Brit. phycol. Bull. **2**, 291—306.

— 1966: *Euglena:* A new look with the electron microscope. Adv. Sci. **23**, 22—37.

— 1982: Ultrastructure. In: The biology of *Euglena*, Vol. 3 (BUETOW, D. E., ed.), pp. 1—27. New York: Academic Press.

— MEEUSE, B. J. D., PRINGSHEIM, E. G., 1965: Structure and physiology of *Euglena spirogyra*. I and II. Arch. Mikrobiol. **50**, 68—102.

LOWNDES, A. G., 1936: Flagella movement. Nature (Lond.) **138**, 210—211.

MACKINNON, D. L., HAWES, R. S. J., 1961: An introduction to the study of protozoa, pp. 69—87. London: Oxford Univ. Press.

MIKOLAJCZYK, E., 1972: Pattern of body movements of *Euglena gracilis*. Acta Protozool. **11**, 317—324.

— 1973: Effects of some chemical factors on the euglenoid movement in *Euglena gracilis*. Acta Protozool. **12**, 133—142.

MIKOLAJCZYK, E., 1975: The biology of *Euglena ehrenbergii* Klebs. I. Fine structure of pellicular complex and its relation to euglenoid movements. Acta Protozool. **14**, 233—240.

— KUZNICKI, L., 1981: Body contraction and ultrastructure of *Euglena*. Acta Protozool. **20**, 1—24.

PRINGSHEIM, E. G., 1946: The biphasic or soil-water culture method for growing algae and flagellata. J. Ecol. **33**, 193—204.

— 1948: Taxonomic problems in *Euglenineae*. Biol. Rev. Cambridge Philos. Soc. **23**, 46—61.

REYNOLDS, E. S., 1963: The use of lead citrate at high pH as an electron-opaque stain in electron microscopy. J. Cell Biol. **17**, 208—212.

SCHWELITZ, F. D., EVANS, W. R., MOLLENHAUER, H. H., DILLEY, R. A., 1970: The fine structure of the pellicle of *Euglena gracilis* as revealed by freeze-etching. Protoplasma **69**, 341—349.

SPURR, A. R., 1969: A low-viscosity epoxy resin embedding medium for electron microscopy. J. Ultrastruct. Res. **26**, 31—43.

SUZAKI, T., TOYOHARA, A., WATANABE, S., SHIGENAKA, Y., SAKAI, H., 1980: Microtubules in protozoan cells. Continuous transition between microtubules and macrotubules revealed by a newly devised isolation technique. Biomed. Res. **1**, 207—215.

TANENBAUM, S. W., 1978: Cytochalasins: Biochemical and cell biological aspects. In: Frontiers of biology, Vol. 46. Amsterdam-New York: North-Holland.

WARNER, F. D., 1978: Cation-induced attachment of ciliary dynein cross-bridges. J. Cell Biol. **77**, R 19–R 26.

Verleger: Springer-Verlag KG, Mölkerbastei 5, A-1010 Wien. — Herausgeber: Prof. Dr. E. Schnepf, Lehrstuhl für Zellenlehre der Universität Heidelberg, Im Neuenheimer Feld 230, D-6900 Heidelberg, Bundesrepublik Deutschland. — Redaktion: Mölkerbastei 5, A-1010 Wien. — Hersteller: Adolf Holzhausens Nachfolger, Kandlgasse 19-21, A-1070 Wien. — Verlagsort: Wien. — Herstellungsort: Wien. — Printed in Austria.

Offenlegung gem. § 25 Abs. 1 bis 3 Mediengesetz: Unternehmensgegenstand: Verlag von wissenschaftlichen Büchern und Zeitschriften. An der Springer-Verlag GmbH & Co. KG sind beteiligt: Dr. Konrad F. Springer als Kommanditist zu 68,5%, Rösi Joos als Kommanditist zu 26,5%, beide Mölkerbastei 5, A-1010 Wien. Geschäftsführer: Dr. Konrad F. Springer, Ing. Wolfram F. Joos und Mag. Bruno Schweder, alle Mölkerbastei 5, A-1010 Wien.